7 Magnetisation Curve:

Another application of the Ginzburg-Landau theory, which is of practical interest, is to determine the magnetisation curve of the Shubnikov phase, i.e. we restrict ourselves to magnetic fields B between the lower and the upper critical field B_{c1} and B_{c2}: $B_{c1} \leq B \leq B_{c2}$. As the Shubnikov phase is governed by the nucleation of flux lines for increasing magnetic fields, the calculation of the respective magnetisation curve relies upon a deeper understanding of the interaction between the flux lines.

7.1 Interaction Energy Between Flux Lines:

We start with discussing again the spatial dependence of both the magnetic induction $\vec{B}(\vec{r})$ and the superconducting electron current density $\vec{j}_s(\vec{r})$. To this end we contrast the result of the London theory in Chapter 4 with numerical calculations:

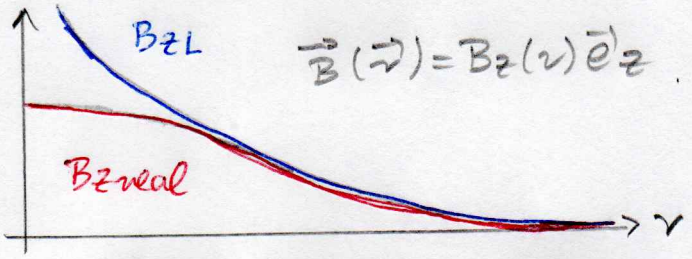

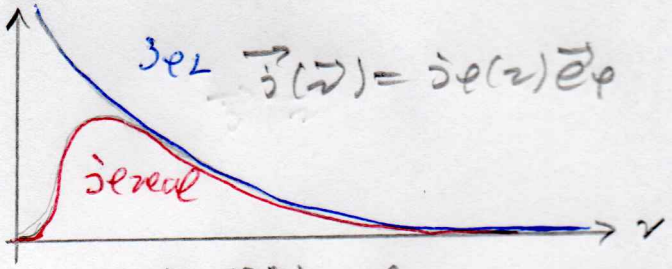

$$B_{zL}(r) \overset{(14.124)}{=\!=} \frac{\phi_0}{2\pi\lambda_L^2} K_0\left(\frac{r}{\lambda_L}\right) \quad (7.1) \qquad j_\varphi(r) \overset{(14.125)}{=\!=} \frac{\phi_0}{\mu_0 2\pi\lambda_L^3} K_1\left(\frac{r}{\lambda_L}\right) \quad (7.4)$$

$$\Rightarrow \begin{cases} \frac{\phi_0}{2\pi\lambda_L^2} \ln\frac{\lambda_L}{r}\,; & r \ll \lambda_L \quad (7.2) \\ \frac{\phi_0}{2\pi\lambda_L^2} e^{-\frac{r}{\lambda_L}}\,; & r \gg \lambda_L \quad (7.3) \end{cases} \Rightarrow \begin{cases} \frac{\phi_0}{\mu_0 2\pi\lambda_L^3} \frac{\lambda_L}{r}\,; & r \ll \lambda_L \quad (7.5) \\ \frac{\phi_0}{\mu_0 2\pi\lambda_L^3} e^{-\frac{r}{\lambda_L}}\,; & r \gg \lambda_L \quad (7.6) \end{cases}$$

Thus, the London theory predicts for both fields a divergence at the center of a flux quantum, whereas the numerical results do not reveal any divergency. Now we discuss the consequences of such spatial dependences of the magnetic induction and the superconducting electron current densities for the energies of a single flux line.

7.1.1 Energies of London Theory:

We recall the energy of the London theory worked out in chapter 4. At first we have to take into account

the energy density of the magnetic field itself

$$e_m(\vec{r}) = \frac{1}{2\mu_0}\vec{B}(\vec{r})^2 \qquad (7.7)$$

Secondly, the superconducting electrons have a kinetic energy density

$$e_s(\vec{r}) \overset{(5.35)}{=\!=} \frac{e_s^2 n_s}{2m_s}\vec{A}(\vec{r})^2 \qquad (7.8)$$

Taking into account the London equation (4.33), the Oersted law (5.56), and the London penetration length (4.47), the kinetic energy density of the superconducting electrons (7.8) reduces to

$$e_s(\vec{r}) = \frac{\lambda_L^2}{2\mu_0}(\mathrm{rot}\,\vec{B})^2 \qquad (7.9)$$

Adding both energy densities (7.7) and (7.9) leads to the following energy within the realms of the London theory

$$E = \frac{1}{2\mu_0}\int dV\left\{\vec{B}(\vec{r})^2 + [\mathrm{rot}\,\vec{B}(\vec{r})]\right\} \qquad (7.10)$$

7.1.2 Self-Energy of Flux Line:

In subsection 6.3.8 we have evaluated the volume integral (7.10) for a single flux line, see (6.65). To this end we have introduced a cut-off cylinder, whose volume was excluded from the volume of integration. As a result we have obtained with (6.72) the self-energy of a flux line per length:

$$\varepsilon_L = \frac{\pi}{\mu_0}\left(\frac{\Phi_0}{2\pi\lambda_L}\right)^2 \ln\frac{\lambda_L}{\xi} \qquad (7.11)$$

In type II superconductors we have $\varkappa = \lambda_L/\xi > 1$, so the line self-energy (7.11) is positive. This means that it is necessary to invest energy in order to create a flux line.

7.1.3 Interaction Energy Between Two Flux Lines:

Now we extend the calculations in subsection 6.3.8 and deal with two flux lines. To this end we proceed like in (6.65) – (6.67) and get from (7.10):

$$E = \frac{1}{2\mu_0}\int_V dV\,\vec{B}\cdot(\vec{B} - \lambda_L^2\Delta\vec{B}) + \frac{\lambda_L^2}{2\mu_0}\oint_{\partial V}(\vec{B}\times\mathrm{rot}\,\vec{B})\cdot d\vec{F} \qquad (7.12)$$

The centers of two flux quanta are assumed to be located at $\vec{r}_1$ and $\vec{r}_2$, respectively. The whole magnetic induction $\vec{B}$ is additive with respect to the magnetic inductions $\vec{B}_1$ and $\vec{B}_2$ from both flux quanta provided they are sufficiently far away from each other:

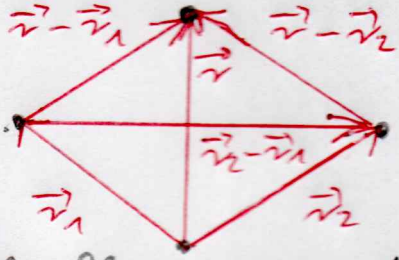

$$\vec{B}(\vec{r}) = \vec{B}_1(\vec{r}-\vec{r}_1) + \vec{B}_2(\vec{r}-\vec{r}_2) \qquad (7.13)$$

The London equation for a flux quantum (4.94) is then correspondingly generalized for two flux quanta

$$\vec{B}(\vec{r}) - \lambda_L^2 \Delta \vec{B}(\vec{r}) = \Phi_0 \vec{e}_z \{\delta^{(2)}(\vec{x}-\vec{x}_1) + \delta^{(2)}(\vec{x}-\vec{x}_2)\} \qquad (7.14)$$

Inserting (7.14) in (7.12) yields

$$E = \frac{\Phi_0}{2\mu_0}\int_V dV\, \vec{B}(\vec{r})\cdot\vec{e}_z\left[\delta^{(2)}(\vec{x}-\vec{x}_1)+\delta^{(2)}(\vec{x}-\vec{x}_2)\right] + \frac{\lambda_L^2}{2\mu_0}\oint_{\partial V}(\vec{B}\times \operatorname{rot}\vec{B})\cdot d\vec{F} \qquad (7.15)$$

If one would insert also here the London expression (7.1) for the magnetic induction $\vec{B}$ in the volume integrals in (7.15), one would obtain logarithmic divergencies. Therefore, we follow the notion of subsection 6.3.8 and introduce now two cut-off cylinders, one around each flux line with radius ξ:

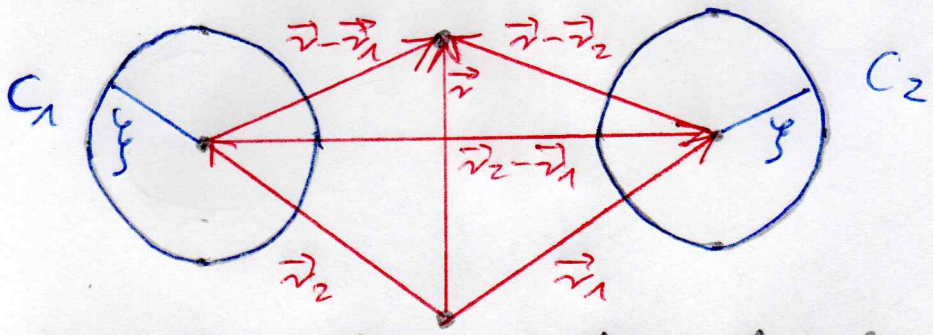

Performing the volume integral over $V = \mathbb{R}\setminus\{C_1, C_2\}$ has the consequence that the centers of both flux quanta are excluded. Therefore, the volume integral in (7.15) then vanishes and only the remaining surface integral has to be performed:

$$E = \frac{\lambda_L^2}{2\mu_0}\oint_{\partial V}(\vec{B}\times\operatorname{rot}\vec{B})\cdot d\vec{F} \qquad (7.16)$$

Inserting (7.13) into (7.16) leads in total to 8 terms:

$$E = \frac{\lambda_L^2}{2\mu_0}\oint_{\partial V}\left[(\vec{B}_1+\vec{B}_2)\times\operatorname{rot}(\vec{B}_1+\vec{B}_2)\right]\cdot(d\vec{F}_1+d\vec{F}_2) \qquad (7.17)$$

Due to the symmetry of the problem the 8 terms decompose into 3 different categories:

1) The first category corresponds to the 2 self-energies of both flux quanta:

$$E_1 = \frac{\lambda_L^2}{2\mu_0}\left\{\oint_{\partial V_1}(\vec{B}_1 \times \operatorname{rot}\vec{B}_1)\cdot d\vec{F}_1 + \oint_{\partial V_2}(\vec{B}_2 \times \operatorname{rot}\vec{B}_2)\cdot d\vec{F}_2\right\} \quad (7.18)$$

Thus, we obtain twice the result of (7.11) for the corresponding line energy

$$\varepsilon_1 = 2\varepsilon_L \overset{(7.11)}{=\!=} \frac{2\pi}{\mu_0}\left(\frac{\phi_0}{2\pi\lambda_L}\right)^2 \ln\frac{\lambda_L}{\xi} \quad (7.19)$$

2) The second category consists of the 4 terms

$$E_2 = \frac{\lambda_L^2}{2\mu_0}\left\{\oint_{\partial V_1}\left[(\vec{B}_1+\vec{B}_2)\times\operatorname{rot}\vec{B}_2\right]\cdot d\vec{F}_1 + \oint_{\partial V_2}\left[(\vec{B}_1+\vec{B}_2)\times\operatorname{rot}\vec{B}_1\right]\cdot d\vec{F}_2\right. \quad (7.20)$$

Here we can show that these terms vanish in limit of a vanishing coherence length, i.e. $\xi \to 0$:

$$\lim_{\xi\to 0}\left|\oint_{\partial V_1}(\vec{B}_1\times\operatorname{rot}\vec{B}_2)\cdot d\vec{F}_1\right| \overset{(7.2)}{\leq} \lim_{\xi\to 0}\left\{\frac{2\pi\xi_L\phi_0}{2\pi\lambda_L^2}\ln\frac{\lambda_L}{\xi}\cdot\left|\operatorname{rot}\vec{B}_2(\vec{r}_1-\vec{r}_2)\right|\right\}\to 0 \quad (7.21)$$

$$\lim_{\xi\to 0}\left|\oint_{\partial V_1}(\vec{B}_2\times\operatorname{rot}\vec{B}_2)\cdot d\vec{F}_1\right| \leq \lim_{\xi\to 0} 2\pi\xi_L\left|\vec{B}_2(\vec{r}_1-\vec{r}_2)\times\operatorname{rot}\vec{B}_2(\vec{r}_1-\vec{r}_2)\right|\to 0 \quad (7.22)$$

Thus, we conclude

$$\lim_{\xi\to 0}\varepsilon_2 = 0 \quad (7.23)$$

3) The third category contains the remaining 2 terms:

$$E_3 = \frac{\lambda_L^2}{2\mu_0}\left\{\oint_{\partial V_1}(\vec{B}_2\times\operatorname{rot}\vec{B}_1)\cdot d\vec{F}_1 + \oint_{\partial V_2}(\vec{B}_1\times\operatorname{rot}\vec{B}_2)\cdot d\vec{F}_2\right\} \quad (7.24)$$

An evaluation in the limit $\xi\to 0$ yields due to (5.56) and taking into account (7.5)

$$\lim_{\xi\to 0} E_3 = \frac{\lambda_L^2}{2\mu_0}\lim_{\xi\to 0} 2\pi\xi_L\mu_0\frac{\phi_0}{\mu_0 2\pi\lambda_L^3}\frac{\lambda_L}{\xi}\left[\vec{B}_1(\vec{r}_1-\vec{r}_2)+\vec{B}_2(\vec{r}_1-\vec{r}_2)\right]$$

$$\overset{(7.1)}{=\!=} 1\cdot\frac{\phi_0}{\mu_0}\frac{\phi_0}{2\pi\lambda_L^2}2K_0\left(\frac{r_{12}}{\lambda_L}\right) \Rightarrow \varepsilon_{12} = \frac{\phi_0^2}{2\pi\mu_0\lambda_L^2}K_0\left(\frac{r_{12}}{\lambda_L}\right) \quad (7.25)$$

Note that the modified Bessel function $K_0(z)$ is always positive, so the line interaction energy (7.25) is positive. This means that two flux lines repel each other. Furthermore, we remark that for distances between two flux lines r_{12}, which are much larger than the London penetration length λ_L, the interaction energy

decays exponentially with e^{-x_{12}/λ_L} due to (7.3). This is similar to the Yukawa potential in molecular physics, which describes the repulsion of two nuclei.

Thus, in the limit $\xi \to 0$ the line energy for two flux lines results in

$$\varepsilon = 2\varepsilon_L + \varepsilon_{12} \tag{7.26}$$

where the line self-energy ε_L and the line interaction energy ε_{12} are given by (7.11) and (7.25), respectively.

7.2 Magnetization Curve above Lower Critical Field

Above the lower critical field B_{c_1} flux lines emerge for the first time. As there exist only few flux lines, they can distribute themselves over the whole superconductor. Thus on average they have a large distance from each other, which corresponds to the underlying assumption of subsection 7.1.3. Therefore, we can assume above the lower critical field B_{c_1} that the line interaction energy (7.19) is positive and that flux lines repel each other.

7.2.1 Area Density of Flux Lines:

Most often a primitive cell of flux lines is realised in the shape of a hexagon. Provided that the distance between two flux lines is given by L, the question arises how large then the area density of flux lines is.

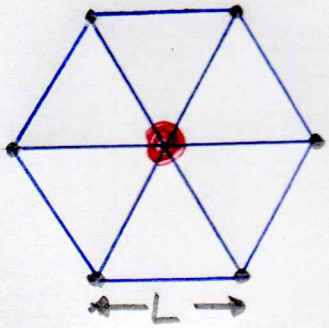

The middle flux line in a hexagon belongs to 6 triangles, i.e. each triangle has the fraction 1/6 of it. But as a triangle is surrounded by 3 flux lines, this yields on average half a flux quantum per triangle. Furthermore, the height of each equilateral triangle amounts to $\sqrt{3}L/2$, so their areas are given by

$$F_\Delta = \frac{1}{2}\frac{\sqrt{3}}{2} L \cdot L = \frac{\sqrt{3}}{4} L^2 \tag{7.27}$$

With these considerations we obtain for the number of flux lines per area

$$n_L = \frac{1/2}{F_\Delta} \overset{(7.27)}{=\!=} \frac{2\sqrt{3}}{3L^2} \tag{7.28}$$

Each flux line captures an elementary flux quan-

tum ϕ_0. This allows to determine from the area densities of flux lines (7.28) the resulting magnetic induction entering the superconductor:

$$B = n_L \phi_0 \qquad (7.29)$$

7.2.2 Basic Idea:

Within the realm of thermodynamics the magnetisation curve follows from minimising the free enthalpy. The Shubnikov phase considered here just above the lower critical field B_{c1} differs energetically from the Meissner phase only insofar as additional flux lines have emerged. The additional free enthalpy per volume for producing these flux lines is given by

$$\Delta g = g_{Shu} - g_{Mei} = \underbrace{n_L \varepsilon_L + \frac{n_L}{2} \sum_{i \neq j} \varepsilon_{ij}}_{=①} \underbrace{- B H}_{=②} \qquad (7.30)$$

Term ① is positive and thus corresponds to an increase of free enthalpy due to the line self-energies of all flux lines and the line interaction energies between two flux lines. Term ② is negative and thus represents a reduction of the enthalpy due to the attractive interaction between the flux lines and the magnetic field.

Note that (7.30) can be considered as a logic extension of the free enthalpy balance set up in subsection 6.3.4. Whereas there we aimed for calculating just the lower critical field B_{c1}, the considerations here allow to determine the magnetisation curve just above the lower critical field B_{c1}.

7.2.3 Calculation of Free Enthalpy Density Difference

Now we focus on the case $B \geq B_{c1}$ with the assumption that $L > \lambda_L$, so together with restriction $\varkappa = \lambda_L / \xi > 1$ we have in total $L > \lambda_L > \xi$. Then we can take advantage of the fast exponential decay of the line interaction energy (7.25) and restrict the summation in (7.30) just to the nearest neighbors.

Thus, let us denote the number of nearest neighbours by the coordination number z. Then we conclude from (7.30):

$$\Delta g = n_L \varepsilon_L + 2 n_L \varepsilon_{12} - B H \qquad (7.31)$$

Inserting (7.29) in (7.31) we get

$$\Delta g = n_L (\varepsilon_L - \phi_0 H) + 2 n_L \varepsilon_{12} \qquad (7.32)$$

Due to (6.52) the line energy ε_L is related to the lower critical field H_{c1}, so (7.32) reduces to

$$\Delta g = n_L \phi_0 (H_{c1} - H) + 2 n_L \varepsilon_{12} \qquad (7.33)$$

Inserting the line interaction energy (7.25), yields

$$\Delta g = n_L \phi_0 (H_{c1} - H) + 2 n_L \frac{\phi_0^2}{2\pi \lambda_L^2} K_0\left(\frac{L}{\lambda_L}\right) \qquad (7.34)$$

so taking into account again (7.29) we get

$$\Delta g = B\left[H_{c1} - H + \frac{2\phi_0}{2\pi \lambda_L^2} K_0\left(\frac{L}{\lambda_L}\right)\right] \qquad (7.35)$$

But the magnetic induction B entering the superconductor and the distance L between two neighbouring flux quanta are not independent from each other. Namely, from (7.28) and (7.29) we read off

$$B = \frac{2\phi_0}{\sqrt{3}\, L^2} \quad \Rightarrow \quad L(B) = \sqrt{\frac{2}{\sqrt{3}}} \sqrt{\frac{\phi_0}{B}} \qquad (7.36)$$

7.2.4 Minimizing Free Enthalpy Difference

Inserting (7.36) into (7.35) yields the free enthalpy difference Δg as a function of the magnetic induction B. The first term

$$\Delta g_1(B) = B(H_{c1} - H) < 0 \qquad (7.37)$$

is attractive just above the lower critical field H_{c1}, where we have $H_{c1} < H$. The second term is of the form

$$\Delta g_2(B) = C_1 B K_0\left(\frac{C_2}{\sqrt{B}}\right) > 0 \qquad (7.38)$$

with some constants C_1, C_2 and is repulsive:

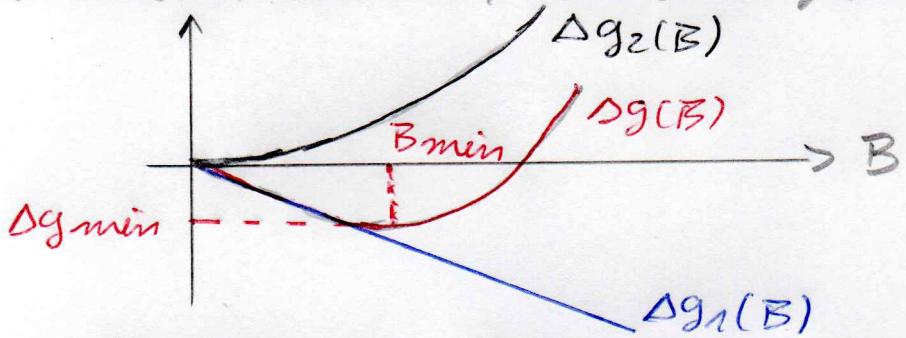

Thus, we have to search for the magnetic induction B_{min}, where the free enthalpy density becomes minimal:

$$\frac{\partial \Delta g(B)}{\partial B} = 0 \qquad (7.39)$$

Writing down (7.35) with (7.36) explicitly we have

$$\Delta g(B) = H_{c1}B - BH + \frac{2\Phi_0 B}{2\pi\lambda_L^2} K_0\left(\sqrt{\frac{2\Phi_0}{\sqrt{3}B}}\frac{1}{\lambda_L\sqrt{B}}\right) \tag{7.40}$$

However, when performing the minimisation according to (7.39), we have to take into account that the magnetic induction B depends on the magnetic field strength H and vice versa:

$$B = B(H) \quad \Longleftrightarrow \quad H = H(B) \tag{7.41}$$

defining the magnetization curve. Differentiating (7.40) with respect to B by taking into account the dependence (7.41) we get due to (4.116):

$$\frac{\partial \Delta g}{\partial B} = H_{c1} - H - B\frac{\partial H}{\partial B} + \frac{2\Phi_0}{2\pi\lambda_L^2}\left\{K_0\left(\sqrt{\frac{2\Phi_0}{\sqrt{3}B}}\frac{1}{\lambda_L\sqrt{B}}\right) + \sqrt{\frac{2\Phi_0}{\sqrt{3}B}}\frac{1}{2\lambda_L\sqrt{B}}K_1\left(\sqrt{\frac{2\Phi_0}{\sqrt{3}B}}\frac{1}{\lambda_L\sqrt{B}}\right)\right\} \tag{7.42}$$

Thus, imposing (7.39) allows to determine the slope of the demagnetization curve:

$$\frac{\partial B}{\partial H} = \frac{B}{H_{c1} - H + \frac{2\Phi_0}{2\pi\lambda_L^2}\left\{K_0\left(\sqrt{\frac{2\Phi_0}{\sqrt{3}B}}\frac{1}{\lambda_L\sqrt{B}}\right) + \sqrt{\frac{2\Phi_0}{\sqrt{3}B}}\frac{1}{2\lambda_L\sqrt{B}}K_1\left(\sqrt{\frac{2\Phi_0}{\sqrt{3}B}}\frac{1}{\lambda_L\sqrt{B}}\right)\right\}} \tag{7.43}$$

Approaching the Meissner phase within the Shubnikov phase amounts to the limit $H \to H_{c1}$, which corresponds to the limit $B \to 0$. Performing the limit $B \to 0$ in (7.43), the arguments of both modified Bessel functions become large, and in this limit they both go over into one and the same exponential function, see top of page 59:

$$\lim_{B\to 0}\frac{\partial B}{\partial H} = \lim_{B\to 0}\frac{B}{\frac{2\Phi_0}{2\pi\lambda_L^2}\sqrt{\frac{\pi}{2\sqrt{\frac{2\Phi_0}{\sqrt{3}}}\frac{1}{\lambda_L\sqrt{B}}}}\left(1 + \sqrt{\frac{2\Phi_0}{\sqrt{3}}}\frac{1}{2\lambda_L\sqrt{B}}\right)e^{-\sqrt{\frac{2\Phi_0}{\sqrt{3}}}\frac{1}{\lambda_L\sqrt{B}}}} \tag{7.44}$$

As an exponential function decays faster than any polynomial can grow, we finally conclude from (7.44)

$$\lim_{B\to 0}\frac{\partial B}{\partial H} = \infty \tag{7.45}$$

Due to (2.6)–(2.8) magnetic induction B, magnetic field strength H and magnetization M are related via

$$B = \mu_0(H + M) \tag{7.46}$$

Thus, a differentiation of (7.46) with respect to H yields

$$\frac{\partial B}{\partial H} = \mu_0 + \mu_0\frac{\partial M}{\partial H} \tag{7.47}$$

and from (7.45) we then read off

$$\lim_{H \to H_{c1}} \frac{\partial M}{\partial H} = \infty \qquad (7.48)$$

This means that the magnetisation curve $M(H)$ has a vertical tangent at the lower critical field $H = H_{c1}$. Thus, considering the Shubnikov phase just in the immediate vicinity of the lower critical field, a type II superconductor behaves magnetically like a type I superconductor:

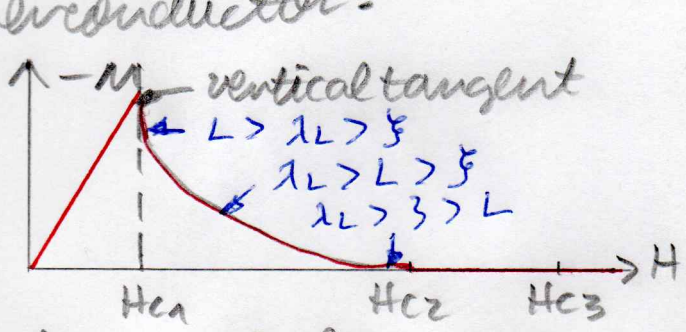

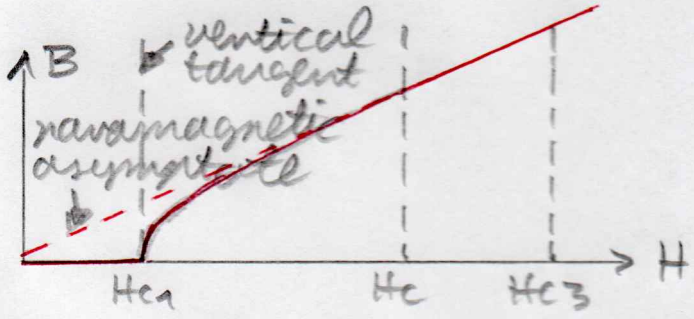

such a vertical tangent at the magnetisation curve can be observed for a perfect single crystal, where no defects exists.

Where we have considered here the region $L > \lambda_L > \xi$, the other regions $\lambda_L > L > \xi$ and $\lambda_L > \xi > \xi$ below the upper critical field H_{c2} are not accessible with the simple model presented here. There the flux lines are no longer far away from each other, in fact that is the regime where they start to overlap. In order to describe that region just below the upper critical field H_{c2} one needs a more elaborate approach based on the Ginsburg-Landau equations, see Chapter 6 of P. G. de Gennes, Superconductivity of Metals and Alloys. For instance, it follows that the magnetisation M, indeed, vanishes at the upper critical field H_{c2}, so the transition there is of second order.